

# High-Throughput Kinase Profiling: A More Efficient Approach toward the Discovery of New Kinase Inhibitors

Chandrasekhar V. Miduturu,<sup>1,8,9</sup> Xianming Deng,<sup>1,8</sup> Nicholas Kwiatkowski,<sup>1</sup> Wannian Yang,<sup>2</sup> Laurent Brault,<sup>3</sup> Panagis Filippakopoulos,<sup>4</sup> Eunah Chung,<sup>5</sup> Qingkai Yang,<sup>6</sup> Juerg Schwaller,<sup>3</sup> Stefan Knapp,<sup>4</sup> Randall W. King,<sup>5</sup> Jiing-Dwan Lee,<sup>6</sup> Sanna Herrgard,<sup>7</sup> Patrick Zarrinkar,<sup>7,9</sup> and Nathanael S. Gray<sup>1,\*</sup>

<sup>1</sup>Department of Biological Chemistry and Molecular Pharmacology, Harvard Medical School and Department of Cancer Biology, Dana-Farber Cancer Institute, Boston, MA 02115, USA

<sup>2</sup>Weis Center for Research, Danville, PA 17822, USA

<sup>3</sup>Department of Biomedicine, University Hospital Basel, 4031 Basel, Switzerland

<sup>4</sup>Structural Genomics Consortium, Nuffield Department of Clinical Medicine and Department of Clinical Pharmacology, University of Oxford, OX3 7DQ Oxford, UK

<sup>5</sup>Department of Cell Biology, Harvard Medical School, Boston, MA 02115, USA

<sup>6</sup>Department of Immunology and Microbiological Science, The Scripps Research Institute, La Jolla, CA 92037, USA

<sup>7</sup>Ambit Biosciences, San Diego, CA 92121, USA

<sup>8</sup>These authors contributed equally to this work

<sup>9</sup>Present address: Blueprint Medicines Corp, Cambridge, MA 02142, USA

\*Correspondence: [Nathanael.Gray@dfci.harvard.edu](mailto:Nathanael.Gray@dfci.harvard.edu)

DOI 10.1016/j.chembiol.2011.05.010

## SUMMARY

Selective protein kinase inhibitors have only been developed against a small number of kinase targets. Here we demonstrate that “high-throughput kinase profiling” is an efficient method for the discovery of lead compounds for established as well as unexplored kinase targets. We screened a library of 118 compounds constituting two distinct scaffolds (furan-thiazolidinediones and pyrimido-diazepines) against a panel of 353 kinases. A distinct kinase selectivity profile was observed for each scaffold. Selective inhibitors were identified with submicromolar cellular activity against PIM1, ERK5, ACK1, MPS1, PLK1-3, and Aurora A,B kinases. In addition, we identified potent inhibitors for so far unexplored kinases such as DRAK1, HIPK2, and DCAMKL1 that await further evaluation. This inhibitor-centric approach permits comprehensive assessment of a scaffold of interest and represents an efficient and general strategy for identifying new selective kinase inhibitors.

## INTRODUCTION

The success of Imatinib mesylate (Schiffer, 2007) as the first small molecule targeted kinase inhibitor for use in cancer therapy, validated protein kinases as important drug targets in the treatment of human diseases (Cohen, 2002). The ubiquitous presence of protein kinases in virtually all signal transduction networks provides a clear impetus for the development of small molecules that can modulate their activity. Indeed, protein

kinases along with G protein coupled receptors constitute the most actively pursued classes of drug target. The protein kinase family constitutes the largest gene-family ever to be tackled for therapeutic development and hence there is an urgent need to develop methodologies that will allow for the rapid discovery and optimization of compounds that can both serve as pharmacological probes to validate the relevance of a particular kinase as well as to serve as “lead” compounds for further drug development activities. In addition, the majority of the kinome has not been targeted with an inhibitor with a useful level of selectivity and therefore there is a need to develop useful tool compounds for these kinases.

Traditional kinase inhibitor discovery approaches have concentrated on a single kinase at a time (Collins and Workman, 2006). These approaches usually involved performing a high-throughput screen using biochemical and cellular assays (Wesche et al., 2005), screening kinase-directed compound libraries (Ding et al., 2002; Li et al., 2004), structure-guided design (Dubinina et al., 2007), and fragment-based assembly methods (Müller et al., 2010). In these methods, the initial “hits” are evolved using iterative rounds of structure-activity relationship (SAR) guided optimization against a single kinase target of interest. Selectivity and potency against other kinases are assessed during the optimization process. As a result, cross-reactivities against other kinases are only discovered serendipitously. The most important drawback is that this traditional “linear” method of discovery has to be repeated for each new kinase target of interest. There is no easy way to ascertain the scope of a scaffold series against the entire kinome. These target-driven methods are therefore low-throughput and time-consuming.

Profiling inhibitor libraries against the entire enzyme class of mammalian serine hydrolases has been recently shown with great success (Bachovchin et al., 2010). A high-throughput kinome-profiling of kinase-directed libraries has been proposed

as a more efficient alternative method to discover novel kinase inhibitors (Goldstein et al., 2008). Kinome-profiling is a “compound-centric” rather than target-centric method in that it seeks to discover what the full range of kinase-targets for a particular compound class are rather than simply what compounds can target any particular kinase. Several assays with a collection of kinases in a variety of formats have been previously reported (Bain et al., 2007; Bantscheff et al., 2007; Cohen, 2010; Fedorov et al., 2007; Karaman et al., 2008). With steady technological improvements, several large scale kinase screening campaigns employing large libraries of compounds have been reported. In one study, 60 Ser/Thr kinases were screened against 156 commercially available compounds (Fedorov et al., 2007) whereas in another study, 577 compounds of various chemical scaffolds were screened against 203 kinases using the Ambit kinase platform (Bamborough et al., 2008). In a most recent study, >20,000 compounds representing many undisclosed structural classes were screened against 317–402 kinases in the ambit kinase platform (Posy et al., 2010). Many of these methods were primarily used to annotate the selectivity of established inhibitors rather than in a primary screening approach to discover new inhibitors of established and novel kinases. In this report, we demonstrate how high-throughput kinome-profiling can be used to screen an entire library of 118 compounds against >60% of the human kinome thereby providing a global survey of the utility of a particular chemical scaffold. We utilized the largest kinase collection available at Ambit Biosciences (353 kinase panel; <http://www.kinomescan.com/>) to screen two unique scaffolds across the entire kinome. Distinct examples from each scaffold were then biologically characterized and developed as useful tool compounds for PIM1, ERK5, ACK1, MPS1, PLK, and Aurora kinases.

## RESULTS

### Utilizing Novel Scaffolds for High-Throughput Kinase Inhibitor Discovery

In this study, two type I kinase inhibitors scaffolds were explored (Zhang et al., 2009). The first scaffold class were the furan thiazolidinediones that are type I inhibitors based on cocrystal structures with CDK2 kinase (Richardson et al., 2007) and PI3K $\gamma$  kinase (Pomel et al., 2006). Crystallographic studies of these compounds revealed that the thiazolidinedione group forms hydrogen bonds to the catalytic lysine and aspartic acid of the DFG motif thus achieving potent inhibition in the absence of any hydrogen bonds to the kinase hinge-region. A similar coordination of the active site lysine is also found in complexes of the glycyamidine group in the natural product kinase inhibitor Hymenialdisine (Meijer et al., 2000). In this report, we profiled both furan thiazolidinediones that bind in type I fashion as well as compounds that were designed to have the potential to bind as type II (DFG-out) inhibitors (Liu and Gray, 2006). (Figure 1; see Table S4 available online for structures of compounds). The second scaffold class were the pyrimidodiazepines that are type I inhibitors that form a bidendate interaction with the kinase hinge using the pyrimidine ring nitrogen (N1) and the aniline NH (both marked by dashed H-bonds in Figure 1) (Kwiatkowski et al., 2010). The pyrimido diazepine scaffold described here was originally derived from the PLK1 inhibitor BI 2536 (Stegmaier

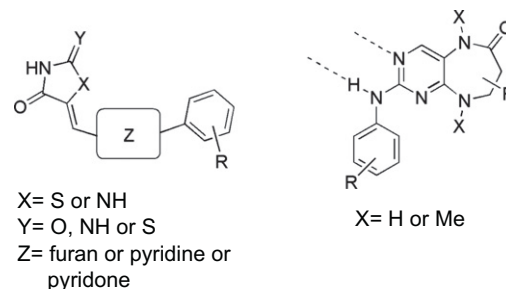


**Figure 1. Chemical Scaffolds Explored in This Study**

The hydrogen bond contacts to the kinase hinge region residues are marked as dashed bonds.

et al., 2007) and BI-D1870 (Sapkota et al., 2007). The expansion of the 6,6-ring system in BI 2536 to a 6,7-ring system to give rise to pyrimido diazepines has been explored before as kinase inhibitors by us and others (Charrier and Durrant, 2010; Gray et al., 2010). In this study, pyrimidodiazepines were explored as a second scaffold series along with a set of pyrimido benzodiazepines that were recently reported as inhibitors of ERK5 kinase (Yang et al., 2010) (see Table S5 for structures of compounds).

### Kinome Spectrum and Selectivity of the Thiazolidinedione-Type Compounds

The thiazolidinediones series were generated in a 2–4 step process from readily available starting materials (see Supplemental Experimental Procedures for synthesis schemes). The common chemical feature among all the compounds in this series is the presence of the thiazolidinedione-like framework at the 2 position of the furan. During the initial stages of this study, other “head” groups such as the barbituric acid, thiobarbituric acid, creatinine, glycyamidine (Wan et al., 2004), pyrazolidinediones, indenediones, imidazolidinediones, and thioimidazolidinones showed little or no interaction to the kinase ATP site. Only the thiazolidinedione-like head groups, which included the rhodanines and iminothiazolidinones showed binding affinity to the ATP site. In general, the iminothiazolidinones were more promiscuous kinase binders than the thiazolidinediones followed by the rhodanines. At the 5-position of the furan core, various substituted phenyl or naphthyl groups were coupled using a Suzuki reaction. In certain cases, anilines were appended to the benzoic acids through an amide linkage. In total, 64 thiazolidinedione-type compounds (including both the non-hinge binding furan-type compounds and the hinge-binding pyridone-type compounds) were screened at 10  $\mu$ M across a 353-kinase panel. The primary screening data for the entire collection of 64 compounds in this scaffold is available in Table S4. About one-third of the total compounds in this set bound strongly to DRK1, HIPK1, and PIM2 kinases (Figure 2A) that suggest that these kinases are likely to be the central targets of this compound class. The primary Ambit screening data were also clustered using the MultiExperiment Viewer (see Experimental Procedures for more details). Clustering the primary screening data provided an opportunity to correlate structural features of the inhibitors and kinome selectivity. In order to facilitate the analysis, an arbitrary cutoff score of 5%

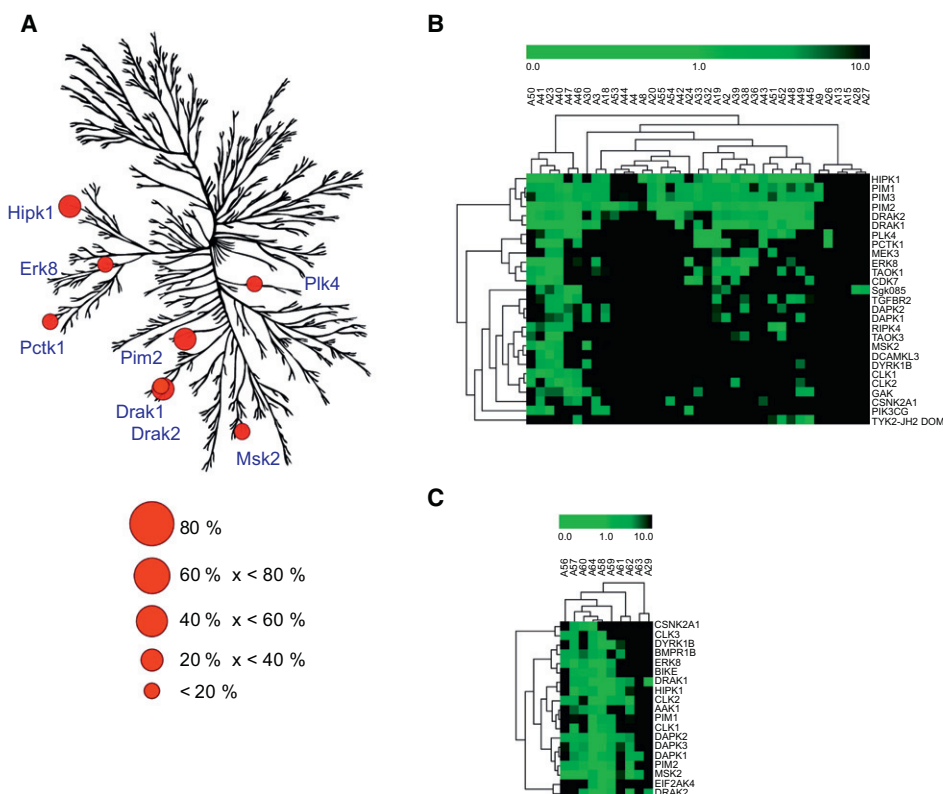


**Figure 2. Kinases Targeted by the Furan and Pyridone Thiazolidinedione-Type Compounds**

(A) Percent of kinases targeted by this scaffold (64 compounds) with an Ambit score of <1% of the DMSO control are highlighted in red circles. The size of the circle represents the percentage of compounds that target a particular kinase. DRAK1 is the most highly targeted kinase with 28% followed by HIPK1 and PIM2 at 27%. Only targeted kinases of 10% and higher are indicated.

(B and C) The primary ambit data for all the (B) furan-type compounds and (C) pyridone-type compounds were clustered using MultiExperiment Viewer. Only kinases with at least three compound hits and with a score of <5% of DMSO control were considered for this clustering analysis. Kinome Illustration reproduced courtesy of Cell Signaling Technology ([www.cellsignal.com](http://www.cellsignal.com)).

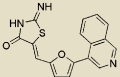
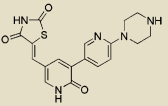
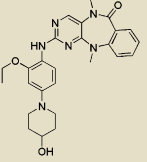
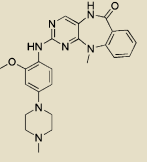
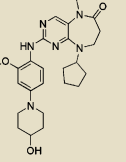
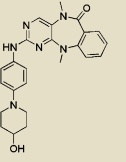
of DMSO control and at least three compound hits for a kinase were chosen (Figures 2B and 2C). The less selective compounds clustered separately to the left and pointed to functional groups (such as an ortho-hydroxy functional group on the phenyl group in compounds A50 and A23) that impart promiscuous recognition of the ATP-site through a putative hinge contact. A few compounds with the furan core replaced with a phenyl, thiazole or a pyridone core were also prepared. Whereas the phenyl core compounds (A21 and A20) yielded few hits, the thiazole core compound (A30), was less selective and less potent on a number of targets. The hinge-binding pyridone compounds were clustered separately as this small set of compounds exhibited a slightly different spectrum of kinase targets (Figure 2C). This set of pyridones was less selective than the non-hinge binding furan compounds with overlapping targets of DRAK1, HIPK1, and PIM2 in addition to new targets such as MSK2 (RPS6KA4) and the DAPK family of kinases.

#### Furan Thiazolidinediones as PIM Kinase Inhibitors

The high-throughput kinase profiling revealed that the furan thiazolidinediones bound strongly to the PIM family of kinases. In vitro biochemical assays were performed in parallel to determine the most potent tool compound (see Table S1 for SAR anal-

ysis). Although a number of furan thiazolidinedione-like compounds exhibited potent inhibition of PIM1 and PIM2 in biochemical assays, many of the compounds with lower computed logP values were not active in cellular assays presumably due to poor membrane penetration (data not shown). We were able to obtain compounds with robust cellular activity by increasing the logP of the compounds. Compound A47 that possessed an IC<sub>50</sub> of 49 nM for inhibiting biochemical activity of both PIM1 and PIM2 emerged as the most promising compound from this set and was chosen for further characterization. Moreover, A47 is the first inhibitor that is equipotent on all three isoforms of PIM kinase (*K<sub>d</sub>* of 40, 23 and 13 nM on PIM 1, 2, and 3, respectively). In addition to binding potently to the fingerprint kinases of this series, A47 also bound strongly to other kinases like Aurora B (29 nM) and Aurora C (154 nM), TGFBR4, and GAK kinases (Table 1; Figure S1A). Compounds that possessed a putative hinge contact also targeted a subset of these kinases. Following previous characterization of other potential small molecule PIM kinase inhibitors (Pogacic et al., 2007), the compound was characterized for its biological activity. First, similar to the imidazo[1,2-b]pyridazine K00135, A47 also significantly impaired survival of murine Ba/F3 cells transformed to IL-3 independence by overexpression of PIM1

**Table 1. Tool Compounds Elaborated from Each Scaffold**

Compound ID	A47	A64	B46	B19	B13	B54
Structure						
Key kinase $K_d$ (nM)	PIM1: 40 PIM2: 23 PIM3: 13	HIPK2: 9.5	ERK5: 80	ACK1: 15	MPS1: 26	Aur A/B/C: –
Key kinase $IC_{50}$ (nM)	PIM1: 49 PIM2: 49 PIM3: –	HIPK2: 74	ERK5: –	ACK1: –	MPS1: 145	Aur A: 8 Aur B: 24 Aur C: 41
Off-targets ( $K_d/IC_{50}$ ) (nM)	Aur B: 210/29  Aur C: –/154  MYLK4: 55/–	CSNK2A2: 6.1/– DAPK1: 9.5/– DYRK1A: 8.8/19 DYRK1B: –/62 HIPK2: 9.5/74 PIM3: 3.7/–	DCAMKL1: 97/–	BRK: 37/47  FRK: 96/264  GAK: 270/– TNK1: 110/–	GAK: 140/–  PLK1: 61/–	TAOK2: –/54.3  MAP3K2: –/155 MAP3K3: –/120
S(10)	0.21	0.16	0.014	0.03	0.011	0.1

Tool compounds elaborated from each scaffold for PIM 1/2, HIPK2, ERK5, ACK1, MPS1, and Aurora kinases are shown.  $K_d$  and  $IC_{50}$  values for the target kinase and select off-target kinases are indicated. Selectivity scores (S(10)) for each compound were calculated as described before (Karaman et al., 2008). See also Figures S1–S6 for whole kinome interaction map of the key compounds as well as complete list of available  $K_d$ s or  $IC_{50}$ s.

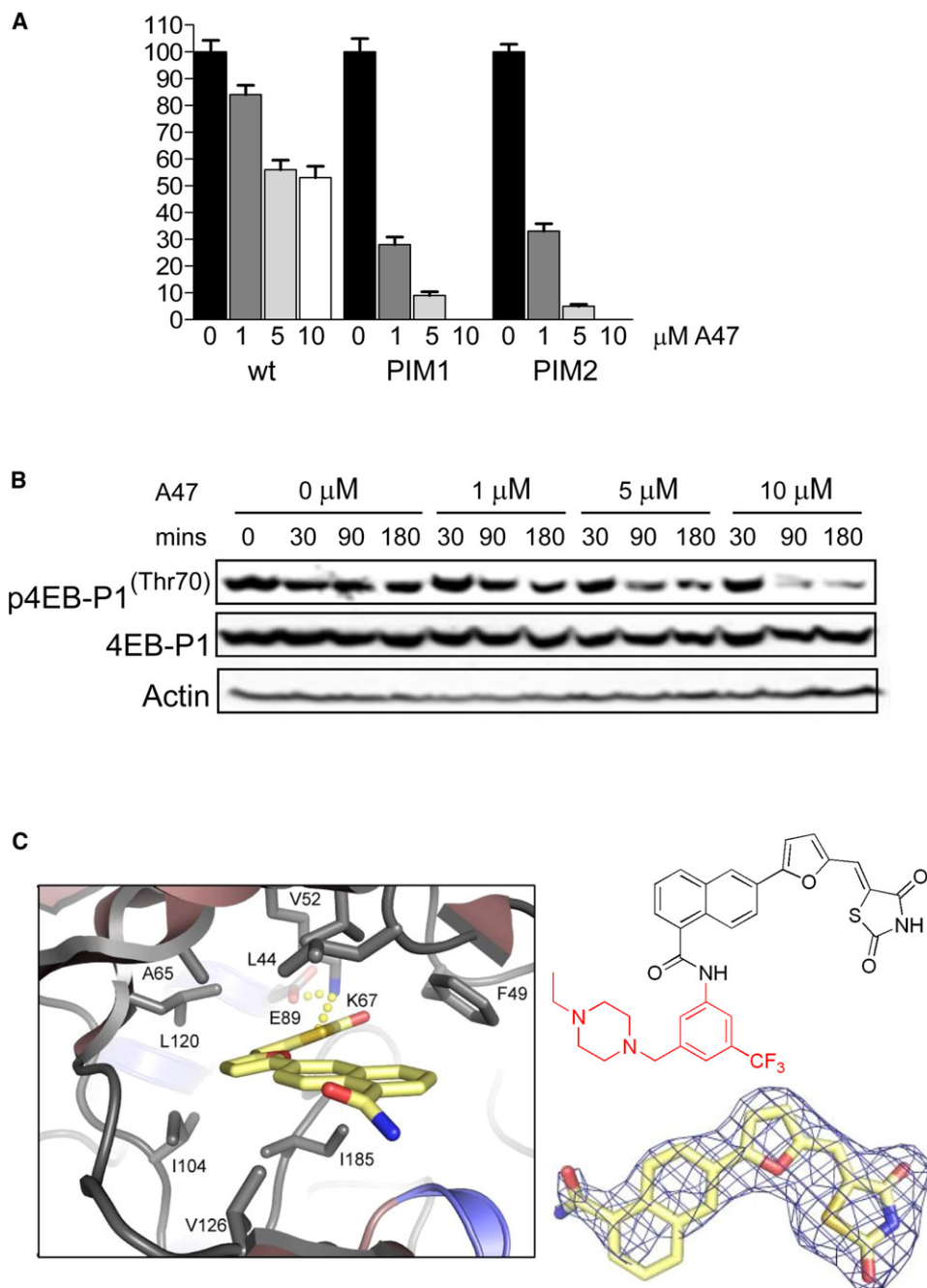


**Figure 3. Cellular Data for the PIM1 Inhibitor A47**

(A) Ba/F3 wild-type (WT) cells and stably expressing hPIM1 and/or hPIM2 cells were exposed to increasing amounts of A47 and cell viability was determined 24 hr and 48 hr later (expressed as a percentage normalized to viability of cells treated with 0.1% DMSO only ( $n = 3$ ). Data is shown for cell viability after 24 hr.

(B) MV4-11 cells were incubated with increasing concentrations of A47 for indicated times, harvested, and protein extracts separated by SDS-PAGE. The effect of the compound on PIM endogenous target was followed by western blotting with indicated phospho-specific antibodies. Membranes were stripped and re-probed with nonphospho-specific and anti-actin antibodies to check for equal loading.

(C) View of cocrystal structure between PIM1 kinase and furan thiazolidinedione A54. The inhibitor binds in a typical type I fashion and its trifluoromethylaniline portion is directed toward the solvent exposed region.

or PIM2 (Figure 3A). Second, A47 impaired survival of a panel of human acute leukemia cells that is associated with an impaired phosphorylation of known PIM substrates such as 4EB-P1 in a time- and dose-dependent fashion (Figure 3B; Figure S1B).

Moreover, A47 also potentially blocked migration of Ba/F3 cells overexpressing PIM1 toward CXCL12 gradient (Figure S1B), demonstrating its inhibitory potential against PIM1 as this kinase have been proposed to be a regulator of CXCR4 function



(Grundler et al., 2009). These observations suggest that A47 has potential anticancer activities in part mediated by its activity toward PIM1. We attempted to crystallize A47 but failed to obtain diffraction quality crystals. The binding mode of a related furan thiazolidinedione compound A54 that contained a “type II” chemical structure to induce a “DFG-out” conformation of the activation loop was solved at 2.2 Å against PIM1 kinase (Figure 3C; see Table S6 for data collection and refinement statistics). A54 is a weak inhibitor of PIM1/2 ( $IC_{50}$  of 774 and 814 nM, respectively) but possessed a much better selectivity profile across the whole kinome than A47. In addition, A54 also inhibited cell proliferation in PIM1 transformed Ba/F3 cells (data not shown). However contrary to the design strategy, the furan thiazolidinedione scaffold bound in a typical “type I” fashion to the PIM1 kinase with a conformation similar to the inhibitors cocrystallized with  $PI3K\gamma$  (Pomel et al., 2006) and cdk2 (Richardson et al., 2007). The trifluoromethylaniline portion of the inhibitor was partially visible in the electron density and was directed to the solvent exposed region instead of toward the hydrophobic pocket created by the DFG-out conformation that is defining feature of a type II inhibitor. The inhibitor made key hydrogen bond interactions between the nitrogen of the thiazolidinedione ring and the catalytic lysine K67 (3.0 Å) as well as the back bone NH of DFG aspartate D186 (3.6 Å). The furan and naphthyl rings made hydrophobic interactions with several hydrophobic residues in the ATP site. The exocyclic carbonyl made a weak interaction with the side chain of D186 (3.9 Å). We speculate that the replacement of this carbonyl with an imino group (as in the lead PIM inhibitor A47) could afford extra stabilization by interacting with the side chain of D186. A superimposed model of the lead inhibitor A47 on the PIM1/A54 complex structure is included in the supplementary information (Figure S1C).

#### Novel Inhibitors of HIPK1/HIPK2 Kinase

A structure-activity relationship study was performed in parallel with high-throughput kinase profiling on a small set of compounds from the pyridone thiazolidinediones (see Table S2) using an in vitro biochemical assay by measuring inhibition of immunoprecipitated HIPK2 activity as well as enzymatic  $IC_{50}$  values (SelectScreen kinase profiling assay) to determine the most potent compounds. Compound A64 was the most potent compound with an  $IC_{50}$  of 74 nM to emerge from this effort. Because HIPKs have roles in cell cycle regulation (Iacovelli et al., 2009; Trapasso et al., 2009), we decided that it was important for a putative HIPK2 inhibitor not to influence Cdk1 activity. The inhibition of the compounds on Cdk1 was also measured using an in vitro MPF kinase assay (see Supplemental Experimental Procedures). A64 was not an effective Cdk1 inhibitor ( $IC_{50} > 10 \mu M$ ). A64 was moderately selective across the kinome (Table 1; Figure S2). Efforts to determine the on-target cellular activity of the compound against HIPK2 were not pursued as robust cellular assays to evaluate the role of this kinase are not yet reported.

#### Kinome Spectrum and Selectivity of the Pyrimido Diazepine and Benzodiazepine Compounds

A pyrimido diazepine and pyrimido benzodiazepine series was synthesized from a 2,4-dichloropyrimidine (see Supplemental

Experimental Procedures for synthesis schemes). Various members of pyrimido diazepines were generated by appending different anilines at the C2 position of the pyrimidine as well as introducing alkylated amides in the diazepine ring. In addition, pyrimido benzodiazepines were synthesized by incorporating an anthranilic acid into the 7-membered ring. In total, 52 compounds including 12 pyrimido benzodiazepines were screened at 10  $\mu M$  against a 353-kinase panel. The primary screening data for the entire collection of 52 compounds in this scaffold is available in Table S5. ERK5 (also known as BMK1), PLK1 and 3, and DCAMKL1 and 2 were the most frequently targeted kinases (Figure 4A; 10%–25% of the compounds). As expected, based on the structural similarity to the BI-2536 PLK1,2,3 inhibitor, the pyrimido diazepines retained binding to PLK1 and PLK3 (PLK2 not assayed) but several additional kinases such as TTK (MPS1) and GAK were targeted by a subset of these compounds. In contrast, fusing an anthranilic acid to the 7-membered ring abolished binding to the PLK kinase family and the other hits obtained for the pyrimido diazepines. Instead, the most frequent targets of the pyrimido benzodiazepines were ERK5 and DCAMKL1 and 2. The clustering data (Figure 4B) clearly indicated the target cluster of the pyrimido benzodiazepines separated from the diazepines. However, the target selectivity of pyrimido benzodiazepines depends on certain distinct structural features that are possessed only by a subset of compounds. Pyrimido benzodiazepines such as B50 and B51 without aniline at the C2 of the pyrimidine did not display the ERK5 and DCAMKL1 and 2 kinase target set. In addition, compounds such as B48 and B49 with a reverse amide at the C5 of the pyrimidine hit very few targets across the kinome. Compounds with a bulky isopropoxy group at the ortho position of the aniline attached to the C2 of the pyrimidine B23 lost the pyrimido benzodiazepine target cluster activity. Similarly, any substitution at this same position completely removed activity against the Aurora kinases suggesting a low tolerance for groups protruding toward the hinge region of the kinase pocket. Methylation of the amide group controlled a tight selectivity factor between the kinases TNK1 and ACK1 (also known as TNK2) (B20 versus B19). Even though only a small set of pyrimido benzodiazepines were profiled in this study (12 compounds), selective and potent inhibitors were obtained and characterized in detail for ERK5 (Yang et al., 2010), ACK1, and Aurora kinases. In addition, a potent and selective pyrimido diazepine inhibitor for MPS1/PLK1 (Kwiatkowski et al., 2010) is also described.

#### Novel Inhibitors for ERK5 Kinase

A structure-activity guided optimization of compounds was performed using a cellular ERK5 autophosphorylation assay (Deng et al., 2011) in parallel with high-throughput kinase profiling. Compound B46 was selected as the compound that displayed the optimal combination of selectivity and cellular potency (Yang et al., 2010). The whole kinome interaction map of B46 against a panel of 402 kinases indicated that B46 binds to only four kinases with a score of <5% of DMSO control (Figure S3).  $K_d$  determination confirmed the binding to ERK5 at 80 nM in addition to DCAMKL1 (97 nM) and DCAMKL2 (190 nM) (Table 1). From this data, it was clear that B46 possesses remarkable selectivity for ERK5 across the entire kinome with a  $K_d$  of <100 nM

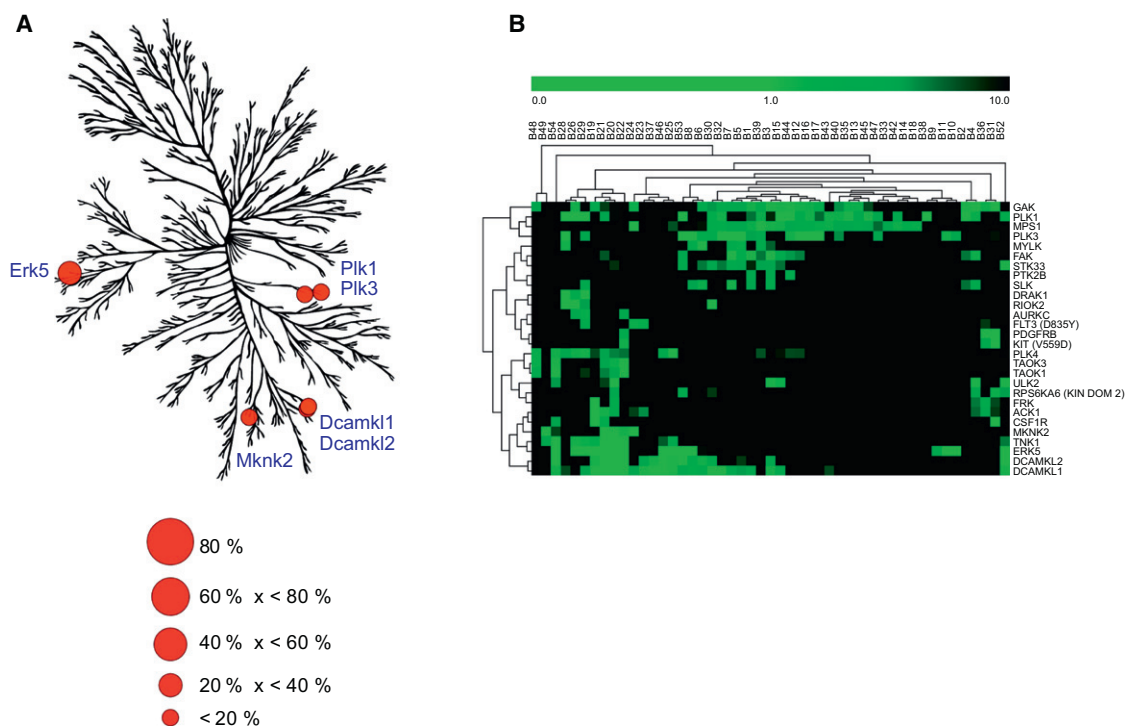


**Figure 4. Kinases Targeted by the Pyrimido Diazepines and Pyrimido Benzodiazepines**

(A) Percent of kinases targeted by the pyrimido diazepines and pyrimido benzodiazepines with an Ambit score of <1% of DMSO control are highlighted in red circles. The size of the circle represents the percentage a particular kinase is targeted. ERK5 is the most highly targeted kinase with 23% followed by PLK3 and DCAMK1 at 15%. Only targeted kinases of 8% and higher are indicated.

(B) The primary ambit data was clustered using MultiExperiment Viewer. Only kinases with at least three compound hits and with a score of <5% of DMSO control were considered for this clustering analysis. Kinome Illustration reproduced courtesy of Cell Signaling Technology ([www.cellsignal.com](http://www.cellsignal.com)).

for only 2 of 402 kinases. The on-target cellular activity of B46 was tested by inhibition of ERK5 autophosphorylation in HeLa cells induced by EGF stimulation (Figure 5A) (Yang et al., 2010).

#### Novel Inhibitors for ACK1 Kinase

From the primary screening data, of the cluster of kinases that were sensitive to the pyrimido benzodiazepine scaffold, only ACK1 and GAK have a threonine as the gatekeeper (other kinases such as TNK1 and ERK5 have a methionine as the gatekeeper). This suggested an H-bond interaction between the threonine side chain and the amide NH on the diazepine ring that could be used as a filter to develop selective inhibitors for ACK1. A homology model constructed using the X-ray crystal structure of ACK1 with debromohymenialdisine (Lougheed et al., 2004) also supported this observation. An SAR study was performed by measuring the binding interaction of a series of compounds against ACK1 using in vitro kinase assays (SelectScreen Kinase Profiling Service) (data not shown; X.D., unpublished data). Compound B19 was the most potent and selective compound among this series with a  $K_d$  of 15 nM against ACK1 (Table 1; Figure S4). B19 was tested for inhibition of kinase activity of ACK1 evaluated by monitoring EGF-induced autophosphorylation in HEK293 cells (Figure 5B). The autophosphorylation was abolished at 2  $\mu$ M concentrations of B19 (lane 3) whereas much less inhibitory effect was observed at 10  $\mu$ M of B20 (lane 4), a compound with methylated diazepine amide in

B19, indicating that the diazepine amide in B19 determines the binding specificity to ACK1. Interestingly cotransfection of a GTPase defective mutant of Cdc42, Cdc42Q61L, which activates ACK1 kinase, recovered part of inhibitory effect of B19 (compare lane 7 with lane 3), suggesting that either Cdc42 competes with the binding site of B19 or Cdc42 caused ACK1 conformational change that reduces the binding affinity to B19. Furthermore, we also tested the effect of B19 on lung cancer A549 cell growth (Figure 5C). At 10  $\mu$ M, B19 completely inhibited the cancer cell growth, and partially inhibited EGF-stimulated cancer cell growth.

#### Novel Dual Inhibitors of MPS1 and PLK1 Kinases

MPS1 emerged as a novel target for the 7-membered ring expanded versions of the dihydropteridinones BI-2536 and BI-D1870 in addition to maintaining reasonable potency against PLK1. A structure-activity relationship study of compounds was performed using in vitro kinase assays (SelectScreen Kinase Profiling Service) in parallel with high-throughput kinase profiling (see Table S3). Compound B13 was selected as the compound that displayed the desired combination of selectivity and potency for MPS1 (Kwiatkowski et al., 2010). The whole kinome interaction map of B13 against a panel of 402 kinases indicated that B13 binds to only 4 kinases with a score of <5% of DMSO control (Figure S5).  $K_d$  determination confirmed the binding to MPS1 at 12 nM in addition to PLK1 (61 nM) and GAK (140 nM)

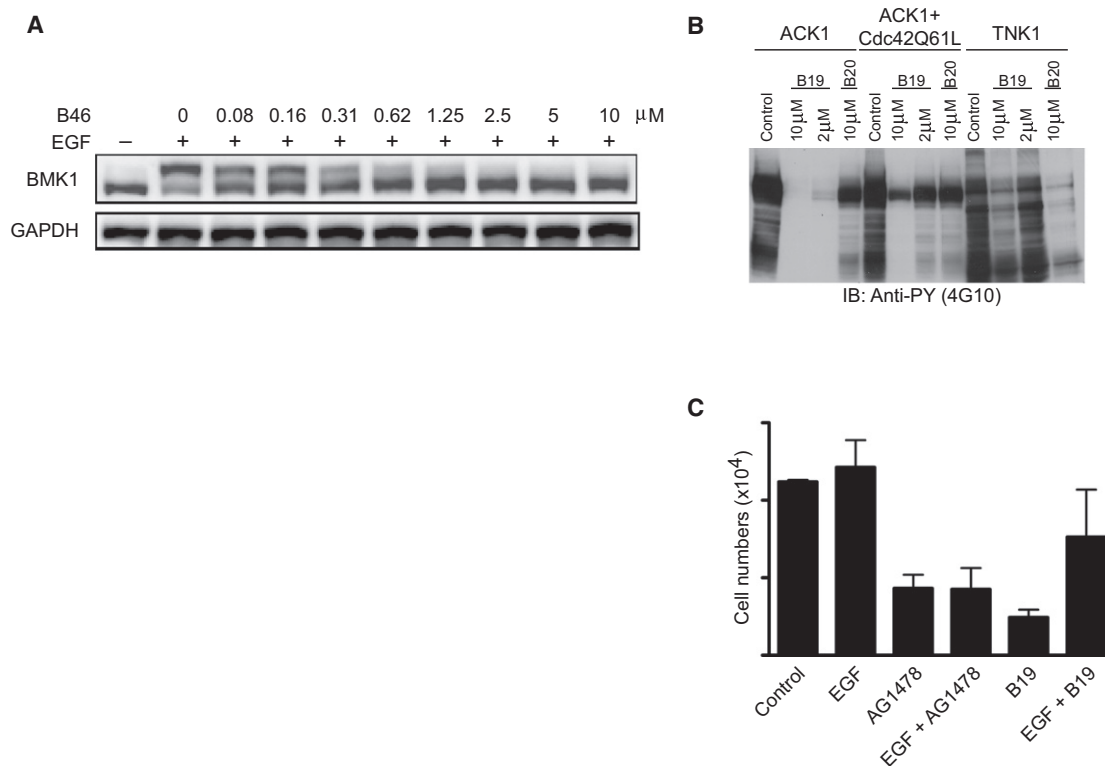


**Figure 5. Cellular Data of the ERK5 Inhibitor B46 and ACK1 Inhibitor B19**

(A) HeLa cells were serum starved overnight followed by treatment with different concentrations of B46 for 1 hr. Cells were then stimulated with EGF for 17 min and BMK1 activation was detected by mobility retardation.

(B) ACK1 or TNK1 cDNA in pcDNA3 vector was transfected into HEK293 cells for 36 hr. DMSO (control), B19 or B20 (N-Me amide version) at indicated concentration was added into the culture medium for 12 hr. The cells were lysed and the cell lysates were subjected to SDS-PAGE. Tyrosine phosphorylated ACK was detected by immunoblotting with anti-phosphotyrosine antibody (4G10).

(C) A549 cells were seeded in a 6-well culture plate at a density of 2000/well. EGF (50 ng/ml), AG1478 (1  $\mu$ M), B19 (10  $\mu$ M), or DMSO (control) was added into culture medium and refreshed every 3 days. The cells were cultured for 7 days and the number of cells was counted with Bright-Line Hemacytometer (Hausser Scientific) under microscope.

(Table 1). The potent binding interaction observed in the initial primary screening at 10  $\mu$ M with Flt3 was not confirmed. From this data, it was clear that B13 possesses remarkable selectivity for MPS1 and PLK1 across the entire kinome with a  $K_d$  of <100 nM for only the 2 of 402 kinases tested. The cellular activity of B13 on MPS1 was tested by assessing the compound's ability to inactivate the spindle assembly checkpoint (SAC), the activity of which requires MPS1 kinase activity (Figures 6A and 6B). Degradation of cyclin B can be used to monitor the progress of the cell through mitosis. The levels of cyclin B accumulate during G2 phase and sustain in the presence of an activated SAC. In U2OS cells, a dose-dependent drop in cyclin B levels was observed in the presence of B13 that could be reversed by the addition of the proteasome inhibitor MG132 (Figure 6B).

#### Novel Inhibitors Targeting Aurora Kinases

Intracellular screening of a select set of pyrimido benzodiazepines identified compounds having SAC inhibitory activity as assessed by the ability of the compounds to bypass a Taxol-induced mitotic arrest. Profiling of these compounds against a panel of 402 kinases showed that they lacked activity against MPS1, a checkpoint kinase targeted by the pyrimido diazepine

B13. This result was consistent with existing SAR data of these compounds that demonstrated that substitutions at positions  $\alpha$ ,  $\beta$  to the carbonyl moiety abolished the ability to inhibit MPS1. Compound B54 was shown to have SAC inhibitory activity at concentrations as low as 50 nM (Figure S6B). Further inspection of the profiling data revealed a modest Ambit binding score for B54 against Aurora B (primary screening score of 1.4 at 1  $\mu$ M screening; Figure S6A for whole kinome interaction map for B54). Subsequent *in vitro* kinase assays supported this assertion demonstrating that B54 had biochemical  $IC_{50}$  of 8 nM, 24 nM, and 41 nM for Aurora A, B, and C, respectively (Table 1). Treatment of U2OS cells with B54 demonstrated a dose-dependent decrease in Aurora A and B autophosphorylation and of Histone H3 ser10 phosphorylation, a known substrate for Aurora B (Figure 6C). At concentrations of 250 nM and above, the formation of monopolar spindles was observed, an indicator of Aurora A inhibition (Figure S6B).

#### DISCUSSION

Traditional kinase inhibitor discovery is a low-throughput process not optimized to efficiently annotate the inhibitory



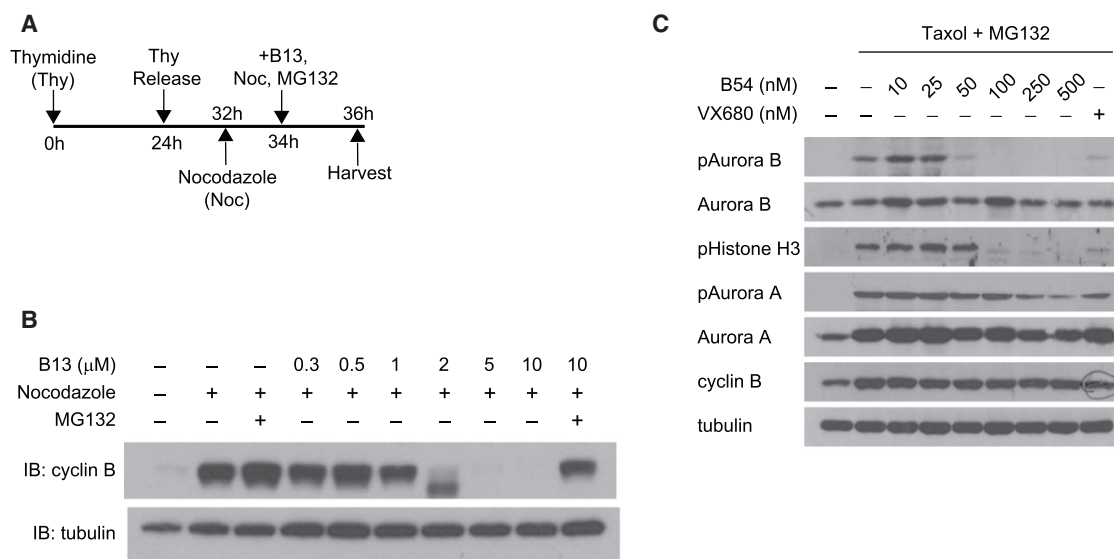


**Figure 6. Cellular Data of the Dual MPS1/Polo-Like Kinases Inhibitor B13 and Pan-Aurora Kinase Inhibitor B54**

(A) Schematic of the treatment regimen used to assess the effect of B13 treatment on spindle checkpoint-induced mitotic arrest in U2OS cells.

(B) Immunoblot of cyclin B from U2OS cells treated with B13. U2OS cells were arrested in mitosis by combination treatment of thymidine and nocodazole prior to treatment with nocodazole or coadministration with B13 ± MG132 for 2 hr.

(C) Immunoblot of mitotic markers from U2OS cells treated with B54. U2OS cells were arrested in mitosis by combination treatment of thymidine and Taxol prior to treatment with Taxol or coadministration with B54 (or VX-680) ± MG132 for 2 hr.

potential of a given scaffold against the entire kinome. In addition, the vast majority of kinase inhibitor discovery efforts takes place in the pharmaceutical industry and predominantly focuses on well-established kinase targets. Thus, despite the tremendous investments in making new kinase inhibitors, the majority of kinases are still not targeted with an inhibitor with a useful level of selectivity. In order to address this problem, we explored the potential of a high-throughput kinase profiling strategy to rapidly deliver new kinase inhibitors. We chose to investigate two chemical scaffold classes that were previously underexplored in detail as kinase inhibitors. Distinct hits from each of the scaffold series were obtained for established as well as novel kinase targets. Most importantly, tool compounds were elaborated for six different kinases to validate the utility of the high-throughput kinase profiling method. These tool compounds meet the criteria for a chemical probe in order to investigate the activity of a desired kinase of interest (Frye, 2010; Kodadek, 2010). In addition, valuable leads were obtained for established and novel kinases such as DRAK1/2, and DCAMKL1/2 that await further characterization. In this study, one example for the furan thiazolidinediones was characterized in detail as an inhibitor of the PIM kinases. The PIM kinases are attractive targets for targeted cancer therapy as they are aberrantly expressed in prostate cancer and other hematological malignancies (Brault et al., 2010). Many recent publications have detailed the discovery and application of PIM kinase inhibitors (Akué-Gédu et al., 2010; Brault et al., 2010; Chang et al., 2010; López-Ramos et al., 2010; Sliman et al., 2010; Tao et al., 2009). The furan thiazolidinedione PIM kinase inhibitors reported here share the thiazolidinedione-like pharmacophore with the benzylidene thiazolidinediones (Xia et al., 2009). The PIM inhibitor characterized

in this report A47, is potent against all three PIM kinases and displays on-target cellular activity (Figures 3A and 3B). Even though A47 displays only moderate selectivity across the entire kinome, it demonstrates the utility of high-throughput kinase profiling for identifying lead compounds that can be subject to further medicinal chemistry efforts. Based on the cocrystal structure of PIM1 with compound A54 (Figure 3C), the increased promiscuity of the lead PIM inhibitor A47 can be speculated to be due to a possible hinge contact between the backbone NH of the kinase hinge region residues and the isoquinoline nitrogen of the inhibitor. An example from the pyridone thiazolidinediones was elaborated through *in vitro* biochemical assays as an inhibitor for HIPK2 (homeodomain-interacting protein kinase 2). HIPK2 is a Ser-Thr kinase with important roles in cell growth and apoptosis in various cell types, tissues and organisms (Calzado et al., 2007; Rinaldo et al., 2007). HIPK2 has been shown to be a potential tumor suppressor as well as a DNA-damage response modulating kinase by activating the apoptosis pathway through phosphorylation of downstream targets including the tumor suppressor p53 (Puca et al., 2010). Selective and potent inhibitors for HIPK2 are thus extremely valuable in delineating the myriad roles played by HIPK2. We chose to develop tool compounds for a novel kinase such as HIPK2 as no inhibitors are currently available. Inhibitors of other kinases have been shown to cross-react with HIPK2 in a profiling study of Ser-Thr kinases (Bain et al., 2007). The high-throughput profiling method described here was valuable to discover important leads as HIPK2 inhibitors that can be used to interrogate HIPK2 function in cellular experiments. Unfortunately, we were unable to characterize the ability of A64 to target HIPK2 in cells due to a lack of a relevant functional assay. Examples from

both the pyrimido diazepines and pyrimido benzodiazepines were characterized in detail as inhibitors for ERK5, ACK1, MPS1/PLK1, and Aurora A/B. Mitogen-activated protein kinases (MAPKs) are well known to be involved in modulating cellular function and are recognized as important targets in the treatment of cancer (Montagut and Settleman, 2009). The characterization of the detailed biological functions of ERK5 has been hampered by the lack of a potent and selective small molecule ERK5 inhibitor. Recently, a dual MEK5/ERK5 inhibitor has been reported from the indolinone carboxamide class (Tatake et al., 2008). In our study, detailed SAR done in parallel with high-throughput kinome profiling yielded compound B46 as a selective ERK5 inhibitor with potent cellular inhibition of ERK5 autophosphorylation. B46 was used as a pharmacological inhibitor to validate the tumorigenic role of ERK5 and showed efficacy in murine xenograft models (Yang et al., 2010). ACK1 (activated Cdc42 associated kinase also known as TNK2) is a nonreceptor tyrosine kinase and overexpression of ACK1 has been found to correlate with increased invasive phenotype of cancer cells and predisposition of primary tumor cells to metastasis (van der Horst et al., 2005). In addition, activated ACK1 was found to promote prostate cancer progression by androgen receptor phosphorylation (Mahajan et al., 2007). Thus, selective and potent inhibitors of ACK1 are useful in probing the role of ACK1 in cancer. Pyrazolo pyrimidines and Lck kinase inhibitors have been reported as potent ACK1 inhibitors (DiMauro et al., 2007; Kopecky et al., 2008). In our study, detailed SAR supported by the speculated interaction between the diazepine ring amide and the gatekeeper threonine, led to compound B19 as the most potent and selective compound for ACK1. B19 is also one of the most selective kinase inhibitors reported with a measured  $K_d$  of <50 nM against only two kinases across the entire kinome. MPS1 (or TTK) is a dual specificity kinase that plays an important role in ensuring the fidelity of mitosis and its role in the spindle assembly checkpoint (SAC) (Musacchio and Salmon, 2007). A selective small molecule inhibitor of MPS1 is useful in probing the function of MPS1 as well as a potential use in cancer drug discovery targeting mitotic kinase signaling pathways. Prior to the disclosure of compound B13 (Kwiatkowski et al., 2010), there were two MPS1 small molecule inhibitors reported in the literature (Dorer et al., 2005; Schmidt et al., 2005). In this report, high-throughput kinase profiling along with detailed SAR study led to B13 as the most potent and selective MPS1 inhibitor reported thus far. B13 was used to describe the role of MPS1 kinase activity in establishment and maintenance of the SAC and investigate the potential therapeutic value of pharmacological targeting of the SAC (Kwiatkowski et al., 2010 and unpublished work). The human Aurora family of kinases includes three closely related protein kinases Aurora A, B, and C. Each kinase is cell cycle regulated and shows hyperactivation in mitotic cells, but they show distinct localization and functions. In this report, biochemical and intracellular investigation revealed a pyrimido benzodiazepine, B54, to be a potent and selective pan-Aurora kinase small molecule inhibitor. Currently, it remains to be seen whether a selective Aurora A, B, or C inhibitor can be attained based on this scaffold class. Compounds selective for particular Aurora family kinases have been vital to assessing the therapeutic benefit gained from selective pharmacological inactivation of the individual Aurora kinases.

## SIGNIFICANCE

Many kinase inhibitor development programs consist of optimizing previously known kinase inhibitors that were serendipitously discovered to possess activity toward a new kinase-target of interest. High-throughput kinome profiling is an efficient way to discover inhibitors by screening compounds against the entire kinome. Here we have demonstrated that by applying kinome-wide profiling at initial screening-stage one can efficiently annotate all the potential kinase targets for a given scaffold-class of interest. One major advantage of this approach is it circumvents the need to develop and implement a new high-throughput screening campaign for each new kinase of interest. Once the potential kinase binding partners are identified, appropriate enzymatic and cellular assays must be developed to verify whether bona fide inhibitors have been obtained and what the effective cellular concentrations of the inhibitor might be. This is especially true when the broad screen is done at a single high concentration of 10  $\mu$ M and the resulting binding score has only qualitative correlation with what might be an effective cellular concentration of the inhibitor. We have applied this strategy to two different scaffold classes to obtain the kinome wide targets for the furan thiazolidinediones and pyrimido diazepines and have discovered nanomolar to single digit micromolar cellular inhibitors of PIM2, ERK5, ACK1, MPS1, PLK1, and Aurora kinases. Several other potential targets of the inhibitors including DAPK1, DRAK1, and HIPK2 await additional cellular studies. We anticipate that continued application of this approach with diverse ATP-site directed templates will deliver new inhibitors for the majority of the kinome that is still not targeted with inhibitors of useful levels of selectivity.

## EXPERIMENTAL PROCEDURES

### Compounds Preparation and Screening on Ambit Kinase Platform

All compounds were dissolved and stored at  $-20^{\circ}\text{C}$  as DMSO stocks. Compounds were screened at a single concentration of 10  $\mu$ M using binding assays as described previously (Fabian et al., 2005; Wodicka et al., 2010). Briefly, extracts containing kinases (expressed either as T7 phage fusion proteins or DNA-tagged) are incubated with an immobilized bait compound (known inhibitor like staurosporine) and the test compound (at 10  $\mu$ M). Test compounds that displace the immobilized bait compound are detected by quantitative PCR. The results are expressed as the percentage of kinase bound to the bait compound bead relative to a DMSO control (%control). Compounds with high affinity have %control of 0–1 whereas compounds with lower affinity have higher scores. As false positives (and negatives) are observed in single-point concentration assays, it is important to confirm a high affinity interaction by determining the  $K_d$  of binding. Because the determination of the  $K_d$ s of all compound-kinase pairs is not practical, only  $K_d$ s for the most important and relevant ones were tested. Even though the kinome-wide hits analysis was performed only with primary screening data and not with  $K_d$  data, good correlation has been observed by comparison of  $K_d$  data to single concentration results for a given kinase (Bamborough et al., 2008).

### Clustering Data

The primary ambit data was clustered using Multiexperiment viewer v4.3 (<http://www.tm4.org/mev.html>). Hierarchical clustering was done using the following parameters: (1), both the compound IDs and the kinases were clustered; (2), ordering of the leaves were optimized for both the compound IDs as

well as kinases; (3), the default distance metric (Euclidean) was chosen; and (4), average linkage method was used to indicate the cluster to cluster distances.

#### ACCESSION NUMBERS

Coordinates have been deposited in the Protein Data Bank with accession code 3QF9.

#### SUPPLEMENTAL INFORMATION

Supplemental Information includes Supplemental Experimental Procedures, six figures and six tables and can be found with this article online at [doi:10.1016/j.chembiol.2011.05.010](https://doi.org/10.1016/j.chembiol.2011.05.010).

#### ACKNOWLEDGMENTS

We thank Ambit Biosciences KINOMEScan high-throughput kinase selectivity profiling services for screening all the compounds against members of the human kinase. We thank Life Technologies Corporation, SelectScreen Kinase Profiling Service for performing enzymatic biochemical kinase profiling. Funding was provided by NIH grants: CA130876-03, HG005693-02, U54 HG006097-01 (N.S.G.), HD 23696-21 (E.C.), and GM66492 (R.W.K.). The Structural Genomics Consortium is a registered charity (1097737) that receives funds from the Canadian Institutes for Health Research, the Canadian Foundation for Innovation, Genome Canada through the Ontario Genomics Institute, GlaxoSmithKline, Karolinska Institutet, the Knut and Alice Wallenberg Foundation, the Ontario Innovation Trust, the Ontario Ministry for Research and Innovation, Merck & Co., the Novartis Research Foundation, the Swedish Agency for Innovation Systems, the Swedish Foundation for Strategic Research, and the Wellcome Trust. P.Z. and S.H. are former and current employees, respectively, at Ambit Biosciences. The kinase inhibitor profiling service KINOMEScan previously owned by Ambit Biosciences is now part of DiscoveRx Corporation.

Received: January 25, 2011

Revised: April 28, 2011

Accepted: May 2, 2011

Published: July 28, 2011

#### REFERENCES

- Akué-Gédu, R., Nauton, L., Théry, V., Bain, J., Cohen, P., Anizon, F., and Moreau, P. (2010). Synthesis, Pim kinase inhibitory potencies and in vitro anti-proliferative activities of diversely substituted pyrrolo[2,3-a]carbazoles. *Bioorg. Med. Chem.* 18, 6865–6873.
- Bachovchin, D.A., Ji, T., Li, W., Simon, G.M., Blankman, J.L., Adibekian, A., Hoover, H., Niessen, S., and Cravatt, B.F. (2010). Superfamily-wide portrait of serine hydrolase inhibition achieved by library-versus-library screening. *Proc. Natl. Acad. Sci. USA* 107, 20941–20946.
- Bain, J., Plater, L., Elliott, M., Shpiro, N., Hastie, C.J., McLauchlan, H., Klevernic, I., Arthur, J.S., Alessi, D.R., and Cohen, P. (2007). The selectivity of protein kinase inhibitors: a further update. *Biochem. J.* 408, 297–315.
- Bamborough, P., Drewry, D., Harper, G., Smith, G.K., and Schneider, K. (2008). Assessment of chemical coverage of kinome space and its implications for kinase drug discovery. *J. Med. Chem.* 51, 7898–7914.
- Bantscheff, M., Eberhard, D., Abraham, Y., Bastuck, S., Boesche, M., Hobson, S., Mathieson, T., Perrin, J., Rida, M., Rau, C., et al. (2007). Quantitative chemical proteomics reveals mechanisms of action of clinical ABL kinase inhibitors. *Nat. Biotechnol.* 25, 1035–1044.
- Brault, L., Gasser, C., Bracher, F., Huber, K., Knapp, S., and Schwaller, J. (2010). PIM serine/threonine kinases in the pathogenesis and therapy of hematologic malignancies and solid cancers. *Haematologica* 95, 1004–1015.
- Calzado, M.A., Renner, F., Roscic, A., and Schmitz, M.L. (2007). HIPK2: a versatile switchboard regulating the transcription machinery and cell death. *Cell Cycle* 6, 139–143.
- Chang, M., Kanwar, N., Feng, E., Siu, A., Liu, X., Ma, D., and Jongstra, J. (2010). PIM kinase inhibitors downregulate STAT3(Tyr705) phosphorylation. *Mol. Cancer Ther.* 9, 2478–2487.
- Charrier, J.-D., and Durrant, S. (2010). Preparation of pteridinones and pyrimidodiazepinones as therapeutic protein kinase inhibitors. Patent WO2010008459.
- Cohen, P. (2002). Protein kinases—the major drug targets of the twenty-first century? *Nat. Rev. Drug Discov.* 1, 309–315.
- Cohen, P. (2010). Guidelines for the effective use of chemical inhibitors of protein function to understand their roles in cell regulation. *Biochem. J.* 425, 53–54.
- Collins, I., and Workman, P. (2006). New approaches to molecular cancer therapeutics. *Nat. Chem. Biol.* 2, 689–700.
- Deng, X., Yang, Q., Kwiatkowski, N., Sim, T., McDermott, U., Settleman, J., Lee, J.-D., and Gray, N. (2011). Discovery of a 2-amino-5,11-dimethyl-5H-benzo[e]pyrimido-[5,4-b][1,4]diazepin-6(11H)-one as a potent and selective inhibitor of big MAP kinase 1 (BMK1/ERK5). *ACS Med. Chem. Lett.* 2, 195–200.
- DiMauro, E.F., Newcomb, J., Nunes, J.J., Bemis, J.E., Boucher, C., Buchanan, J.L., Buckner, W.H., Cheng, A., Faust, T., Hsieh, F., et al. (2007). Discovery of 4-amino-5,6-biaryl-furo[2,3-d]pyrimidines as inhibitors of Lck: development of an expedient and divergent synthetic route and preliminary SAR. *Bioorg. Med. Chem. Lett.* 17, 2305–2309.
- Ding, S., Gray, N.S., Wu, X., Ding, Q., and Schultz, P.G. (2002). A combinatorial scaffold approach toward kinase-directed heterocycle libraries. *J. Am. Chem. Soc.* 124, 1594–1596.
- Dorer, R.K., Zhong, S., Tallarico, J.A., Wong, W.H., Mitchison, T.J., and Murray, A.W. (2005). A small-molecule inhibitor of Mps1 blocks the spindle-checkpoint response to a lack of tension on mitotic chromosomes. *Curr. Biol.* 15, 1070–1076.
- Dubinina, G.G., Chupryna, O.O., Platonov, M.O., Borisko, P.O., Ostrovskaya, G.V., Tolmachev, A.O., and Shtil, A.A. (2007). In silico design of protein kinase inhibitors: successes and failures. *Anticancer. Agents Med. Chem.* 7, 171–188.
- Fabian, M.A., Biggs, W.H., 3rd, Treiber, D.K., Atteridge, C.E., Azimioara, M.D., Benedetti, M.G., Carter, T.A., Ciceri, P., Edeen, P.T., Floyd, M., et al. (2005). A small molecule-kinase interaction map for clinical kinase inhibitors. *Nat. Biotechnol.* 23, 329–336.
- Fedorov, O., Marsden, B., Pogacic, V., Rellos, P., Müller, S., Bullock, A.N., Schwaller, J., Sundström, M., and Knapp, S. (2007). A systematic interaction map of validated kinase inhibitors with Ser/Thr kinases. *Proc. Natl. Acad. Sci. USA* 104, 20523–20528.
- Frye, S.V. (2010). The art of the chemical probe. *Nat. Chem. Biol.* 6, 159–161.
- Goldstein, D.M., Gray, N.S., and Zarrinkar, P.P. (2008). High-throughput kinase profiling as a platform for drug discovery. *Nat. Rev. Drug Discov.* 7, 391–397.
- Gray, N. S., Deng, X., and Kwiatowski, N. P. (2010). Preparation of pyrimidodiazepinone kinase scaffold compounds and methods of treating disorders. Patent WO2010080712.
- Grundler, R., Brault, L., Gasser, C., Bullock, A.N., Dechow, T., Woetzel, S., Pogacic, V., Villa, A., Ehret, S., Berridge, G., et al. (2009). Dissection of PIM serine/threonine kinases in FLT3-ITD-induced leukemogenesis reveals PIM1 as regulator of CXCL12-CXCR4-mediated homing and migration. *J. Exp. Med.* 206, 1957–1970.
- Iacovelli, S., Ciuffini, L., Lazzari, C., Bracaglia, G., Rinaldo, C., Prodromo, A., Bartolazzi, A., Sacchi, A., and Soddu, S. (2009). HIPK2 is involved in cell proliferation and its suppression promotes growth arrest independently of DNA damage. *Cell Prolif.* 42, 373–384.
- Karaman, M.W., Herrgard, S., Treiber, D.K., Gallant, P., Atteridge, C.E., Campbell, B.T., Chan, K.W., Ciceri, P., Davis, M.I., Edeen, P.T., et al. (2008). A quantitative analysis of kinase inhibitor selectivity. *Nat. Biotechnol.* 26, 127–132.
- Kodadek, T. (2010). Rethinking screening. *Nat. Chem. Biol.* 6, 162–165.
- Kopecky, D.J., Hao, X., Chen, Y., Fu, J., Jiao, X., Jaen, J.C., Cardozo, M.G., Liu, J., Wang, Z., Walker, N.P., et al. (2008). Identification and optimization

- of N3,N6-diaryl-1H-pyrazolo[3,4-d]pyrimidine-3,6-diamines as a novel class of ACK1 inhibitors. *Bioorg. Med. Chem. Lett.* **18**, 6352–6356.
- Kwiatkowski, N., Jelluma, N., Filippakopoulos, P., Soundararajan, M., Manak, M.S., Kwon, M., Choi, H.G., Sim, T., Deveraux, Q.L., Rottmann, S., et al. (2010). Small-molecule kinase inhibitors provide insight into Mps1 cell cycle function. *Nat. Chem. Biol.* **6**, 359–368.
- Li, B., Liu, Y., Uno, T., and Gray, N. (2004). Creating chemical diversity to target protein kinases. *Comb. Chem. High Throughput Screen.* **7**, 453–472.
- Liu, Y., and Gray, N.S. (2006). Rational design of inhibitors that bind to inactive kinase conformations. *Nat. Chem. Biol.* **2**, 358–364.
- López-Ramos, M., Prudent, R., Moucadel, V., Sautel, C.F., Barette, C., Lafanechère, L., Mouawad, L., Grierson, D., Schmidt, F., Florent, J.C., et al. (2010). New potent dual inhibitors of CK2 and Pim kinases: discovery and structural insights. *FASEB J.* **24**, 3171–3185.
- Lougheed, J.C., Chen, R.H., Mak, P., and Stout, T.J. (2004). Crystal structures of the phosphorylated and unphosphorylated kinase domains of the Cdc42-associated tyrosine kinase ACK1. *J. Biol. Chem.* **279**, 44039–44045.
- Mahajan, N.P., Liu, Y., Majumder, S., Warren, M.R., Parker, C.E., Mohler, J.L., Earp, H.S., and Whang, Y.E. (2007). Activated Cdc42-associated kinase Ack1 promotes prostate cancer progression via androgen receptor tyrosine phosphorylation. *Proc. Natl. Acad. Sci. USA* **104**, 8438–8443.
- Meijer, L., Thunnissen, A.M., White, A.W., Garnier, M., Nikolic, M., Tsai, L.H., Walter, J., Cleverley, K.E., Salinas, P.C., Wu, Y.Z., et al. (2000). Inhibition of cyclin-dependent kinases, GSK-3 $\beta$  and CK1 by hymenialdisine, a marine sponge constituent. *Chem. Biol.* **7**, 51–63.
- Montagut, C., and Settleman, J. (2009). Targeting the RAF-MEK-ERK pathway in cancer therapy. *Cancer Lett.* **283**, 125–134.
- Müller, G., Sennhenn, P.C., Woodcock, T., and Neumann, L. (2010). The 'retro-design' concept for novel kinase inhibitors. *IDrugs* **13**, 457–466.
- Musacchio, A., and Salmon, E.D. (2007). The spindle-assembly checkpoint in space and time. *Nat. Rev. Mol. Cell Biol.* **8**, 379–393.
- Pogacic, V., Bullock, A.N., Fedorov, O., Filippakopoulos, P., Gasser, C., Biondi, A., Meyer-Monard, S., Knapp, S., and Schwaller, J. (2007). Structural analysis identifies imidazo[1,2-b]pyridazines as PIM kinase inhibitors with in vitro antileukemic activity. *Cancer Res.* **67**, 6916–6924.
- Pomel, V., Klicic, J., Covini, D., Church, D.D., Shaw, J.P., Roulin, K., Burgat-Charvillon, F., Valognes, D., Camps, M., Chabert, C., et al. (2006). Furan-2-yl-methylene thiazolidinediones as novel, potent, and selective inhibitors of phosphoinositide 3-kinase gamma. *J. Med. Chem.* **49**, 3857–3871.
- Posy, S.L., Hermsmeider, M.A., Vaccaro, W., Ott, K.H., Todderud, G., Lippy, J.S., Trainor, G.L., Loughney, D.A., and Johnson, S.R. (2010). Trends in kinase selectivity: insights for target class-focused library screening. *J. Med. Chem.* **54**, 54–66.
- Puca, R., Nardinocchi, L., Givol, D., and D'Orazi, G. (2010). Regulation of p53 activity by HIPK2: molecular mechanisms and therapeutic implications in human cancer cells. *Oncogene* **29**, 4378–4387.
- Richardson, C.M., Nunns, C.L., Williamson, D.S., Parratt, M.J., Dokurno, P., Howes, R., Borgognoni, J., Drysdale, M.J., Finch, H., Hubbard, R.E., et al. (2007). Discovery of a potent CDK2 inhibitor with a novel binding mode, using virtual screening and initial, structure-guided lead scoping. *Bioorg. Med. Chem. Lett.* **17**, 3880–3885.
- Rinaldo, C., Prodosmo, A., Siepi, F., and Soddu, S. (2007). HIPK2: a multitasked partner for transcription factors in DNA damage response and development. *Biochem. Cell Biol.* **85**, 411–418.
- Sapkota, G.P., Cummings, L., Newell, F.S., Armstrong, C., Bain, J., Frodin, M., Grauert, M., Hoffmann, M., Schnapp, G., Steegmaier, M., et al. (2007). BI-D1870 is a specific inhibitor of the p90 RSK (ribosomal S6 kinase) isoforms in vitro and in vivo. *Biochem. J.* **401**, 29–38.
- Schiffer, C.A. (2007). BCR-ABL tyrosine kinase inhibitors for chronic myelogenous leukemia. *N. Engl. J. Med.* **357**, 258–265.
- Schmidt, M., Budirahardja, Y., Klompmaier, R., and Medema, R.H. (2005). Ablation of the spindle assembly checkpoint by a compound targeting Mps1. *EMBO Rep.* **6**, 866–872.
- Sliman, F., Blairvacq, M., Durieu, E., Meijer, L., Rodrigo, J., and Desmaële, D. (2010). Identification and structure-activity relationship of 8-hydroxy-quinoline-7-carboxylic acid derivatives as inhibitors of Pim-1 kinase. *Bioorg. Med. Chem. Lett.* **20**, 2801–2805.
- Steegmaier, M., Hoffmann, M., Baum, A., Lénárt, P., Petronczki, M., Krssák, M., Gürtler, U., Garin-Chesa, P., Lieb, S., Quant, J., et al. (2007). BI 2536, a potent and selective inhibitor of polo-like kinase 1, inhibits tumor growth in vivo. *Curr. Biol.* **17**, 316–322.
- Tao, Z.F., Hasvold, L.A., Levenson, J.D., Han, E.K., Guan, R., Johnson, E.F., Stoll, V.S., Stewart, K.D., Stamper, G., Soni, N., et al. (2009). Discovery of 3H-benzo[4,5]thieno[3,2-d]pyrimidin-4-ones as potent, highly selective, and orally bioavailable inhibitors of the human protooncogene proviral insertion site in Moloney murine leukemia virus (PIM) kinases. *J. Med. Chem.* **52**, 6621–6636.
- Tatake, R.J., O'Neill, M.M., Kennedy, C.A., Wayne, A.L., Jakes, S., Wu, D., Kugler, S.Z., Jr., Kashem, M.A., Kaplita, P., and Snow, R.J. (2008). Identification of pharmacological inhibitors of the MEK5/ERK5 pathway. *Biochem. Biophys. Res. Commun.* **377**, 120–125.
- Trapasso, F., Aqeilan, R.I., Iuliano, R., Visone, R., Gaudio, E., Ciuffini, L., Alder, H., Paduano, F., Pierantoni, G.M., Soddu, S., et al. (2009). Targeted disruption of the murine homeodomain-interacting protein kinase-2 causes growth deficiency in vivo and cell cycle arrest in vitro. *DNA Cell Biol.* **28**, 161–167.
- van der Horst, E.H., Degenhardt, Y.Y., Strelow, A., Slavin, A., Chinn, L., Orf, J., Rong, M., Li, S., See, L.H., Nguyen, K.Q., et al. (2005). Metastatic properties and genomic amplification of the tyrosine kinase gene ACK1. *Proc. Natl. Acad. Sci. USA* **102**, 15901–15906.
- Wan, Y., Hur, W., Cho, C.Y., Liu, Y., Adrian, F.J., Lozach, O., Bach, S., Mayer, T., Fabbro, D., Meijer, L., and Gray, N.S. (2004). Synthesis and target identification of hymenialdisine analogs. *Chem. Biol.* **11**, 247–259.
- Wesche, H., Xiao, S.H., and Young, S.W. (2005). High throughput screening for protein kinase inhibitors. *Comb. Chem. High Throughput Screen.* **8**, 181–195.
- Wodicka, L.M., Ciceri, P., Davis, M.I., Hunt, J.P., Floyd, M., Salerno, S., Hua, X.H., Ford, J.M., Armstrong, R.C., Zarrinkar, P.P., and Treiber, D.K. (2010). Activation state-dependent binding of small molecule kinase inhibitors: structural insights from biochemistry. *Chem. Biol.* **17**, 1241–1249.
- Xia, Z., Knaak, C., Ma, J., Beharry, Z.M., McInnes, C., Wang, W., Kraft, A.S., and Smith, C.D. (2009). Synthesis and evaluation of novel inhibitors of Pim-1 and Pim-2 protein kinases. *J. Med. Chem.* **52**, 74–86.
- Yang, Q., Deng, X., Lu, B., Cameron, M., Fearn, C., Patricelli, M.P., Yates, J.R., 3rd, Gray, N.S., and Lee, J.D. (2010). Pharmacological inhibition of BMK1 suppresses tumor growth through promyelocytic leukemia protein. *Cancer Cell* **18**, 258–267.
- Zhang, J., Yang, P.L., and Gray, N.S. (2009). Targeting cancer with small molecule kinase inhibitors. *Nat. Rev. Cancer* **9**, 28–39.